HHS Public Access

Author manuscript

Free Radic Biol Med. Author manuscript; available in PMC 2015 October 01.

Published in final edited form as:

Free Radic Biol Med. 2014 October ; 75: 230–240. doi:10.1016/j.freeradbiomed.2014.07.021.

Oxidative stress-mediated activation of extracellular signal-regulated kinase contributes to mild cognitive impairment-related mitochondrial dysfunction

Xueqi Gan[1,2], **Long Wu**[1], **Shengbin Huang**[1,2], **Changjia Zhong**[1], **Guangyue Li**[1,2], **Haiyang Yu**[2], **Russell Howard Swerdlow**[3], **John Xi Chen**[4], and **Shirley ShiDu Yan**[1,*]

[1]Department of Pharmacology and Toxicology, and Higuchi Bioscience Center, School of Pharmacy, University of Kansas, Lawrence, KS66047

[2]State Key Laboratory of Oral Diseases, West China Hospital of Stomatology, Sichuan University, Cheng Du, China 610041

[3]Department of Neurology, University of Kansas Medical Center, Kansas City, KS66160

[4]Department of Neurology, Memorial Sloan-Kettering Cancer Center, 1275 York Avenue, New York, NY 10065, USA.

Abstract

Mild cognitive impairment (MCI) occurs during the pre-dementia stage of Alzheimer's disease (AD) and is characterized by a decline in cognitive abilities that frequently represents a transition between normal cognition and AD dementia. Its pathogenesis is not well understood. Here, we demonstrate the direct consequences and potential mechanisms of oxidative stress, mitochondrial dynamic and functional defects in MCI-derived mitochondria. Using cytoplasmic hybrid (cybrid) cell model in which mitochondria from MCI or age-matched non-MCI subjects were incorporated into a human neuronal cell line depleted of endogenous mitochondrial DNA, we evaluated the mitochondrial dynamics and functions, as well as the role of oxidative stress in the resultant cybrid lines. We demonstrated increased expression levels of mitofusin 2 (Mfn2) is markedly induced by oxidative stress in MCI-derived mitochondria along with aberrant mitochondrial functions. Inhibition of oxidative stress rescues MCI-impaired mitochondrial fusion/fission balance as shown by the suppression of Mfn2 expression, attenuation of abnormal mitochondrial morphology and distribution, and improvement in mitochondrial function. Furthermore, blockade of MCI related

*Corresponding author: Shirley ShiDu Yan M.D, Departments of Pharmacology and Toxicology and Higuchi Bioscience Center, School of Pharmacy, University of Kansas, 2099 Constant Ave. Lawrence, KS 66047, USA, shidu@ku.edu, Tel: 1-785-864-3637.

Author contributions

Shirley Shidu Yan directed and designed research, and wrote the paper; Xueqi Gan conducted experiments, analyzed data, and wrote the paper; Long Wu, Shengbin Huang, Changjia Zhong and Guangyue Li conducted experiments and analyzed data; Haiyang Yu, Russel Howard Swerdlow, and John Xi Chen contributed to experimental design and writing.

Conflict of Interest

The authors have no conflict of interest to disclose.

stress-mediated activation of extracellular signal-regulated kinase (ERK) signaling not only attenuates aberrant mitochondrial morphology and function but also restores mitochondrial fission and fusion balance, in particular inhibition of overexpressed Mfn2. Our results provide new insights into the role of the oxidative stress-ERK-Mfn2 signal axis in MCI-related mitochondrial abnormalities, indicating that the MCI phase may be targetable for the development new therapeutic approaches that improve mitochondrial function in age-related neurodegeneration.

Keywords

Mitochondrial fission and fusion; Mild Cognitive Impairment; Oxidative stress; ERK; Mfn2; Cybrid cells

Introduction

Mild cognitive impairment (MCI) is characterized by a decline in cognitive abilities that is noticeable yet not severe enough to completely disrupt an individual's daily activity, and is generally considered to be a transitional phase between normal aging and early dementing disorders, especially Alzheimer's disease (AD) [1–3]. As patients with MCI typically convert to definitive AD (probability of 50% within 4 years or at a rate of about 12% per year) [4, 5], it is important to consider whether targeting early treatment interventions towards MCI patients holds potential merit. Some neuropathologic changes observed in MCI partially overlap with the functional alterations seen in AD; for example, neuritic plaques in neocortical regions and neurofibrillary tangles (NFT) in the temporal lobe are seen in MCI patients [6], and there is significant elevation of oxidative DNA damage in peripheral lymphocytes and brain tissues of MCI patients [7–9]. In addition, several gene mutations associated with AD have been observed in subjects with MCI including polymorphic variation in apolipoprotein E and mutations in presenilin 1 and the amyloid precursor protein [10–13]. Although the underlying mechanisms remain elusive, increasing evidence indicates an essential role for mitochondrial dysfunction in AD etiology and pathology [14]. Interestingly, the impairment of mitochondrial function observed in AD is also seen in MCI subjects; this includes decreased cytochrome *c* oxidase activity [15], decreased mitochondrial membrane potential and lower mitochondrial cytochrome *c* content [16]. Thus, although we know that mitochondrial dysfunction may play a critical role in MCI pathologies and its development into AD, its underlying mechanisms are not well understood.

Mitochondria are dynamic organelles, which engage in repeated cycles of fusion and fission. Mitochondrial dynamics (fission and fusion events) are essential for maintenance of mitochondrial morphology, appropriate distribution and normal function [17, 18]. In mammals, the balance of mitochondrial dynamics is regulated by the large dynamin-related GTPases fusion [mitofusin 1 and 2 (Mfn1 and Mfn2) and optic atrophy1 (OPA1)] and fission proteins [dynamin-like protein (Drp1) and mitochondrial fission 1 protein (Fis1)] [19, 20]. Neurons are particularly reliant on mitochondrial dynamic properties as they require mitochondria in the synaptic terminals [21]. Deficiency in either fission or fusion reduces mitochondrial trafficking, leading to aberrant distribution of mitochondria and

defective cellular function [22, 23]. Disrupted mitochondrial fission/fusion balance is consistently involved in neurodegenerative diseases including AD [24, 25]. Although altered balance of mitochondrial fission/fusion is involved in AD postmortem brain [25, 26], transgenic AD mouse models, and amyloid beta (Aβ)-treated in vitro cell cultures [27, 28], the role of mitochondrial dynamic balance in mediating MCI mitochondrial morphology and function and its underlying mechanisms have not been explored.

In the present study, we determined whether and how mitochondrial alterations occur in MCI-derived mitochondria. Using the cytoplasmic hybrid (cybrid) model in which mitochondria from MCI patients or symptom-free, age-matched non-MCI subjects were incorporated into human neuronal (SH-SY5Y) cells previously depleted of endogenous mitochondrial DNA (mtDNA), we comprehensively evaluated the changes of MCI-specific mitochondrial dynamics and mitochondrial function. Our studies provide substantial evidence that disturbed mitochondrial dynamics and impaired mitochondrial functions contribute to MCI pathology, and may provide an opportunity for developing diagnostic and therapeutic advances.

Material and methods

Human subjects and creation of cybrid cell lines

Human subjects for the MCI and Non-MCI group were recruited from the University of Kansas Alzheimer's Disease Center (KU ADC, 7 MCI patients and 7 age-matched Non-MCI controls). Based on the National Institute of Neurological and Communicative Disorders and Stroke and the Alzheimer's Disease and Related Disorders Association criteria [29], MCI diagnosis was made in accordance with the criteria defined by Petersen et al. [5], and the patients were classified as 0.5 according to the Clinical Dementia Rating (CDR) scale. Non-MCI subjects were without subjective or objective evidence of cognitive impairment. The ages of MCI and Non-MCI subject platelet donors were 72.6+2.5 and 74+3.0 years, respectively. Gender, age and disease status of donor patients are presented in supplemental Table S1. This study was approved by the University of Kansas Medical Center (KUMC) Institutional Review Board. All subjects provided written informed consent to participate in the study.

To create cybrids for this study, Rho^0 SH-SY5Y cells lacking mtDNA were obtained from the KU ADC Mitochondrial Genomics and Metabolism Core and repopulated with mitochondria containing platelet mtDNA from volunteer patients or age-matched controls as previously described [30]. Briefly, Rho^0 cells were incubated with donor platelets in a Dulbecco's Modified Eagle Medium (DMEM)-polyethylene glycol solution. Immediately after this, cells were initially placed in DMEM supplemented with 10% non-dialyzed fetal bovine serum (FBS), 200μg/ml sodium pyruvate, 150μg/ml uridine, and 1% penicillin–streptomycin solution to recover. Seven days after the fusion event, cells were switched to a selection medium containing 10% dialyzed fetal calf serum without pyruvate and uridine. These conditions resulted in selection against Rho0 cells that were not repopulated with donor mitochondria. Only cells containing patient platelet mtDNA can regain aerobic competence and survive the subsequent selection processes. Following selection, each cybrid cell line was maintained in DMEM supplemented with 10% non-dialyzed FBS and

1% penicillin-streptomycin solution in a humidified 95% air, 5% CO2 incubator at 37°C for over 2 months. Quantitative real-time polymerase chain reaction (rPCR) showed that intact mtDNA copies were present in all cybrids without detectable large-scale deletion after many passages of cell proliferation (Fig. S1). Cells were treated with the antioxidant drug probucol (10μM) (Sigma), ERK1/2 inhibitor PD98058 (10 μM) (Sigma) for 24 hours prior to biochemical and molecular assays.

Measurement of enzyme activities associated with respiratory chain complexes and ATP levels

The key enzyme activities associated with the mitochondrial respiratory chain, including complex I (NADH-ubiquinone reductase), complex II (succinate dehydrogenase), complex III (ubiquinol-cytochrome c reductase), complex IV (cytochrome c oxidase, CcO) and citrate synthase, were measured in cybrid cell lysates and isolated platelets' mitochondria as described previously [31–33]. ATP levels were measured using an ATP Bioluminescence Assay Kit (Roche) following the manufacturer's instructions and using a Shimadzu (Kyoto, Japan) UV1200 spectrophotometer.

Oxidative stress, mitochondrial membrane potential, and mitochondrial morphology analysis

Cybrid cells were harvested from 75cm^2 flasks and replated at low density onto Lab-Tek eight-well chamber slides. To estimate production of reactive oxygen species (ROS), 80% confluent cybrid cells were exposed to 2.5μM Mitosox Red, a fluorochrome specific for anion superoxide produced in the inner mitochondrial compartment (Molecular Probes) at 37°C for 30 minutes. To assess mitochondrial membrane potential, cells were co-stained with Mitotracker Green (MTGreen) (100nM; Molecular Probes) and tetramethylrhodamine methyl ester (TMRM) (100nM; Molecular Probes) at 37°C for 30 minutes. Fluorescence from MTGreen is independent of membrane potential, whereas TMRM is sensitive to membrane potential. For visualization of mitochondria, cybrid cells were stained with Mitotracker Red (200nM; Molecular Probes) at 37°C for 30 minutes before fixation.

Leica TCS SPE confocal scanning microscopes with a 63× 1.4 NA Apochrome objective lens (Carl Zeiss MicroImaging, Inc.) were used to photograph cells. Excitation wavelengths were 543 nm for Mitosox, TMRM or Mitotracker Red, and 488 nm for MTGreen, respectively. Post-acquisition processing was performed with MetaMorph (Molecular Devices) and NIH Image J software for quantification and measurement of fluorescent signals to assess mitochondrial length and occupied area. Mitochondrial size, shape, density, and fluorescent intensity were quantified by an investigator blinded to experimental groups. More than 100 clearly identifiable mitochondria from randomly selected 10 to 15 cells per experiment were measured in 3 to 5 independent experiments.

Evaluation of intracellular ROS levels was accessed by election paramagnetic resonance (EPR) spectroscopy as described in our previous study [34–36]. CMH (cyclic hydroxylamine 1-hydroxy-3-methoxycarbonyl-2,2,5,5-tetramethyl-pyrrolidine) (100μM) was added to cybrid cell culture 30 min before the end of the treatments. After treatments, cells were washed with cold PBS, collected, and drawn into glass capillaries. The EPR

spectra were collected, stored, and analyzed with a Bruker EleXsys 540 x-band EPR spectrometer (Billerica, MA) using the Bruker Software Xepr (Billerica, MA).

Isolation of mitochondria and immunoblot analysis

Mitochondrial fraction isolated from cybrid cells were suspended in buffer (150mM KCl, 5mM HEPES, 2mM K_2HPO_4, 5mM glutamate, 5mM malate, 150mM potassium thiocyanate, pH 7.2). Mitochondrial fraction and cell lysate were subjected to immunoblotting. Mouse anti-Mfn2 (1:2000, Sigma), rabbit anti-Drp1 (1:3000, Thermo scientific), rabbit anti-Opa1 (1:5000, Abcam), rabbit anti-Fis1 (1:3000, Abcam), mouse anti-Hsp60 (1:5000, Enzo), rabbit anti-phospho-ERK1/2, mouse anti-ERK1/2 (1:2000, Cell signaling), rabbit anti-PGC1α (1:2000, Santa Cruz) and mouse anti-β-actin (1:8000, Sigma) were used as primary antibodies. Binding sites of primary antibody were visualized with horseradish peroxidase-conjugated anti-rabbit IgG antibody (1:5000, life technology) or anti-mouse IgG antibody (1:5000, life technology) followed by the addition of enhanced chemiluminescence (ECL) substrate (GE Healthcare). Relative quantification of optical density for immune reactive bands was performed using NIH Image J software.

Knockdown of Mfn2 expression by siRNA-Mfn2

Cybrid cells were transfected with siRNA targeting human Mfn2 (accession number NM012062) or control siRNA(ON-TARGET Plus SMART Pool™, Dharmacon Research) using Oligofectamine (Invitrogen) according to the manufacturer's instructions. Mfn2 silencing efficiency was evaluated by immunoblotting and immunostaining of Mfn2 protein expression at 48 hours after siRNA transfection. In parallel experiments, mitochondrial morphology was measured by immunostaining and Mitotracker Red staining.

Statistical analysis

Data are presented as mean ± SEM. Statistical analysis was performed using Statview software (SAS Institute, Version 5.0.1). Differences between means were assessed by Student's t-test or one-way analysis of variance (ANOVA) with Bonferroni-Dunn posthoc test. $P < 0.05$ was considered significant.

Results

Abnormal Mitochondrial Morphology and Mitochondrial Fission/Fusion Events in MCI Cybrid Neurons

Mitochondrial density in whole cell, cell body, and cell processes was lower in MCI cybrid cells compared to non-MCI cells (Fig. 1A1–A3). Morphologically, mitochondria in non-MCI cybrids were rod-like or elongated, and regularly distributed (Fig. 1C), whereas mitochondria were obviously more elongated in MCI cybrids. Mitochondrial length was 1.4 fold longer than non-MCI cybrids in the cell body; this effect was increasingly pronounced with greater distance from nuclei, reaching a 1.7 fold relative increase in the neuronal process area (Fig. 1B1–B4).

Given that normal mitochondrial fusion and fission balance controls the number, length, and tubular shape of mitochondria [37, 38], we tested whether MCI-induced mitochondrial

elongation was mediated by impaired mitochondrial fusion and fission events. Mitochondrial fractions from each cybrid cell line were isolated to assess fission and fusion protein levels by immunoblotting (Fig. 1D–E). As shown in Fig. 1D, compared to non-MCI mitochondrial fractions, Drp1 levels were not significantly changed in mitochondrial fractions of MCI cybrids, however Mfn2, which controls mitochondrial fusion, was increased (1.8 fold) in mitochondria from MCI cybrids (Fig. 1E). In addition, there were no significant differences of Fis1 and Opa1 expression levels between non-MCI and MCI-derived mitochondria (Fig. S2). Thus, in MCI-derived mitochondria alterations in fusion protein levels were shifted in a direction that favors mitochondrial fusion.

Mitochondrial Dysfunction in MCI Cybrid Cells

Because mitochondrial dynamics are important for maintenance of mitochondrial function, we next evaluated mitochondrial function by assessing key enzyme activity associated with respiratory chain activity, mitochondrial membrane potential, and energy production in MCI and Non-MCI cybrid cells. Complex I (NADH-ubiquinone reductase), III (ubiquinol-cytochrome c reductase), and IV (cytochrome c oxidase, CcO) activity (Fig. 2A–C) of MCI cybrids (respectively) decreased by 1.6, 1.5, and 1.3 fold, respectively, as compared to non-MCI cybrids. We did not find significant changes in complex II (succinate dehydrogenase) activity in MCI cybrid cells (Fig. S3A). In parallel, ATP levels in MCI cybrids were significantly lower than in non-MCI cybrids (Fig. 2D). We also examined citrate synthase activity to consider potential differences in mitochondrial enrichment between MCI and non-MCI cybrids. Citrate synthase activity was comparable between groups (Fig. S3B). Differences in mitochondrial mass are therefore unlikely to account for the observed decrease in complex I, III, and IV activities. In addition, we obtained similar results from MCI platelet mitochondria showing deficits in mitochondrial respiratory enzyme activities (Fig. S4). These results validate abnormalities in platelet mitochondria, which occur as early as MCI phase before onset of any symptoms or AD pathology.

Mitochondrial depolarization (reflecting a decreasing membrane potential) resulted in a loss of dye from the mitochondria and decreased mitochondrial fluorescence intensity. The intensity of TMRM staining was significantly decreased in MCI cybrids as compared to non-MCI cybrids (Fig. 2E). The measurement of TMRM staining intensity was normalized to Mitotracker Green fluorescence, the values of which for each group were shown in Fig. S5, indicating that the validated mitochondrial parameters were comparable among groups.

Given that ROS is generated as a by-product of electron transfer through different respiratory chain complexes and that ROS accumulation affects mitochondrial function, we tested whether MCI cybrids have abnormal mitochondrial ROS generation and accumulation by measuring mitochondrial superoxide production with Mitosox Red. Mitosox staining intensity was significantly increased in MCI cybrids compared to non-MCI controls, indicating increased levels of mitochondrial ROS in MCI cybrids (Fig.2F). To further confirm the oxidative stress status of each cybrid cell line, we employed a highly specific EPR assay to quantitatively measure the intracellular ROS levels in Non-MCI and MCI cybrids. As shown in Fig. 2G, H, the intracellular ROS levels were significantly elevated in MCI cybrids compared to non-MCI cybrids. This data in conjunction with the result of

Mitosox suggests an elevation of intracellular ROS production/accumulation in MCI cybrid cells containing MCI-derived mitochondria.

Effect of Antioxidant Treatment on Mitochondrial Morphology, Function, and Fission/Fusion Proteins in MCI Cybrid Cells

Increasing evidence suggests that mitochondrial dysfunction is linked to increased oxidative stress [39]. Here, we exploited the direct effects of antioxidant/scavenger properties of probucol to determine whether antioxidant treatment prevents or reduces mitochondrial dysfunction in MCI cybrid cells. The treatment of Probucol almost abolished ROS production as indicated by reduced Mitosox intensity and EPR values as well as improved mitochondrial membrane potential (Fig. 3A–E) in MCI cybrids as compared to vehicle-treated MCI cybrid cells. Importantly, probucol treatment also significantly restored complex I activity and ATP levels in MCI cybrid cells (Fig. 3F–G). Taken together, these results suggest that antioxidants may benefit MCI-derived mitochondria.

In view of the detrimental effect of oxidative stress on mitochondrial dynamics [40, 41], we then assessed the effect of antioxidant treatment with probucol on mitochondrial density, length, and morphology. Indeed, probucol treatment resulted in significantly increased mitochondrial density and shortened mitochondrial length in MCI cybrid cells compared to vehicle treated cybrids (Fig. 4A–B). Abnormal mitochondrial morphology (elongation) in MCI cybrids was largely reversed compared to vehicle-treated MCI cybrids (Fig. 4C), indicating a protective effect of antioxidant treatment on abnormal mitochondrial morphology. We next investigated mitochondrial fusion protein expression in cybrid cells following probucol treatment. Probucol treatment significantly decreased Mfn2 expression levels, reducing it to the levels found in non-MCI cells (Fig. 4D). These data demonstrate antioxidant-mediated recovery of impaired mitochondrial fission and fusion dynamics in MCI mitochondria.

Activation of ERK signal pathway contributes to defects in mitochondrial fission/fusion dynamics and function in MCI cybrids

Given that oxidative stress induces activation of MAP kinase including extracellular receptor kinase (ERK) [42, 43], we next explored a signal pathway involved in regulation of mitochondrial fission/fusion dynamics and function [42, 44, 45]. ERK1/2 phosphorylation increased by 3–4 folds in MCI cybrids compared to Non-MCI neurons. The addition of PD98059, a specific ERK inhibitor largely abolished ERK1/2 phosphorylation (Fig. 5A). Total ERK1/2 was not significantly changed in MCI cybrids compared to non-MCI cybrids. To determine the effect of oxidative stress on ERK1/2 activation, cells were treated with probucol and then analyzed for phospho-ERK1/2. Probucol treatment inhibited ERK1/2 phosphorylation in MCI cybrid neurons (Fig. 5B), compared to vehicle treatment. Addition of PD98059 to MCI cybrid cells also completely suppressed mitochondrial ROS generation (Fig. 5C) as well as intracellular ROS production measured by EPR (Fig. 5D–E). Although oxidative stress-induced activation of ERK1/2 was described in various types of cells [46, 47], it is less clear whether oxidative stress-activated ERK1/2 signaling pathway contributes to altered mitochondrial dynamics and functions in MCI cybrids. Therefore, we examined whether blockade of ERK1/2 activation rescues mitochondrial dysfunction in MCI cybrid

mitochondria. Mitochondrial membrane potential was significantly increased in MCI cybrid cells in the presence of an ERK1/2 inhibitor (PD980590), as shown by a significantly higher intensity of TMRM staining in MCI cybrid cells than in vehicle-treated cells (Fig. 5F).

We next evaluated mitochondrial morphology and mitochondrial fission/fusion protein expression levels in cybrid cells treated with PD98059 to determine the effect of ERK1/2 signal transduction. Mitochondrial density was increased in MCI cybrid cells treated with PD98059 compared to vehicle-treated cells (Fig. 5G–H). Morphologically, there was a significant reduction in mitochondrial elongation in MCI cybrids (Fig. 5I). Immunoblotting of mitochondrial fractions revealed that PD98059 treatment reduced Mfn2 expression to the levels seen in non-MCI cybrid cells (Fig. 5J). Thus, our data indicate that inhibition of ERK rescues abnormal mitochondrial dynamics responsible for mitochondrial morphology and function.

Mfn2-silencing with siRNA Restores Mitochondrial Function and Mitochondrial Fission/fusion balance in MCI cybrids

To further determine the protective effects of Mfn2 suppression on aberrant mitochondrial morphology and function observed in MCI-derived mitochondria, we reduced Mfn2 expression levels to the non-MCI levels by using siRNA at a selected concentration to eliminate the potential detrimental effect of the lack of Mfn2 [48]. Immunoblotting showed that Mfn2 expression levels were reduced by 50% in siRNA-treated MCI-cybrid cells compared to those treated with unrelated control siRNA (Fig. 6A). Immunostaining with a specific Mfn2 antibody confirmed the suppression of Mfn2 expression in siRNA-treated MCI cybrid cells (Fig. 6B). Notably, abnormal mitochondrial morphology was attenuated by treating with Mfn2-siRNA, as shown by a reduction of mitochondrial elongation in MCI cybrids when compared to control siRNA transfection; MCI cybrids displayed almost normal rod-like mitochondria following Mfn2 siRNA transfection (Fig. 6B). Mitochondrial density and length were significantly increased and decreased, respectively, in Mfn2-siRNA transfected cells as compared to control siRNA transfected cybrids (Fig. 6C–D).

Next, we evaluated mitochondrial function with Mfn2-siRNA and control siRNA treatment. Deficits in complex IV activity, mitochondrial membrane potential, and intracellular and mitochondrial ROS production were reversed by Mfn2-siRNA treatment as compared to control siRNA treatment (Fig. 6E–K). These results indicate that preventing Mfn2 overexpression in MCI-cybrid cells attenuates abnormal mitochondrial morphology and function. Thus, enhanced Mfn2 expression in MCI-derived mitochondria may contribute to abnormal mitochondrial structure and function.

Discussion

Mitochondrial dysfunction has been widely documented in AD brain and AD mouse models [31, 49, 50], but the precise role of such dysfunction in AD remains largely undefined. Using the cybrid model, we demonstrate that mitochondrial defects are also present at the MCI phase, which often represents a prodromal stage of AD. Importantly, we show a potential mechanism in which MCI mitochondria impair mitochondrial fission/fusion events through oxidative stress-mediated ERK1/2 signal activation. We also reveal the

consequences and impact of MCI-derived mitochondrial defects on mitochondrial function in comparison of MCI cybrids with non-MCI cybrids. Consistent with studies performed in MCI subjects [15, 51, 52], we demonstrated impaired mitochondrial respiratory chain enzyme activity, decreased membrane potential, increased mitochondrial and intracellular reactive oxygen species (ROS), and defects in energy metabolism with decreased ATP levels in MCI cybrids. Peroxisome proliferator-activated receptor γ coactivator α (PGC1α), as a key regulator of energy metabolism, plays important role in mediating changes of mitochondrial mass and coupling efficiency[53]. Consistent with the previous study [52], the expression level of PGC1α was significantly reduced in MCI cybrids compared to non-MCI cybrids (Fig. S6). In view of that PGC1α-deficient mice exhibit decreased mitochondrial number and decreased respiratory capacity [54], a decrease in PGC1α expression in MCI-derived mitochondria might account for the altered mitochondrial dynamic and function. Further investigations are required for elucidation of the detailed mechanisms involved in PGC1α and MCI mitochondrial defects.

Mitochondrial functional defects manifest as altered mitochondrial morphology and distribution in MCI cybrids. These lines demonstrate significant changes in mitochondrial morphology and fission/fusion balance. Morphologically, mitochondria in MCI cybrids are larger and less dense than they are in non-MCI cybrids. We explored the involvement of abnormal mitochondrial dynamics by investigating the expression of mitochondrial fission and fusion proteins in MCI cybrids, and found increased Mfn2 levels in MCI cybrid mitochondria. Given that mitochondrial Mfn2 is involved in mitochondrial fusion [25], increased mitochondrial Mfn2 levels in MCI cybrids suggests altered Mfn2 expression likely contributes to enhanced mitochondrial fusion. Indeed, no changes in other mitochondrial fission and fusion markers including Fis1, Opa1, and Drp1 levels were found in MCI cybrids compared to non-MCI cybrid cells. The mitochondrial Fis1 and Opa1 levels remained comparable between MCI and Non-MCI cybrids, which were consistent with the results shown by Silva et al. [52]. Although most of our results were consistent with the observation of the Silva et al. study, we displayed a different mitochondrial dynamic shifted direction. In Silva's study, Drp1 levels of mitochondria trended higher in the MCI cybrid group than the control cybrid group. Drp1 serine 637 phosphorylation was reduced in the MCI group compared with control group. These results supported the author's hypothesis that mitochondrial fission-fusion balance shifted towards increased fission in the MCI cybrids. On the other side, our study clearly showed Drp1 levels in mitochondria were comparable between Non-MCI and MCI groups. Further, we demonstrated for the first time that Mfn2 levels were higher in MCI cybrids than Non-MCI cybrids. Accordingly, changes in mitochondrial morphology were seen in MCI mitochondria as shown as elongated mitochondria. While the impact of MCI-derived mitochondrial defects on mitochondrial function, such as respiratory chain activity is well-proven in our and others' studies, the discrepancy of Drp1 expression levels in MCI-cybrid cells between ours and Silva et al could be ascribed to the methodologies, such as individual patient variation, different methods for mitochondrial isolation, choice of reference proteins, and resources of antibodies. Nerveless, our present studies clearly showed alterations in mitochondrial fusion protein Mfn2 along with mitochondrial morphology MCI-derived mitochondria, which may

be responsible for a shift in a direction that favors mitochondrial fusion as seen in MCI-derived mitochondria.

Perturbations in mitochondrial fusion and fission can lead to distinctive defects in neurons. Mitochondrial fusion likely protects function by facilitating mixing of mitochondrial contents, which results in protein complementation, mtDNA repair and proper distribution of metabolites [55]; however, overly fused mitochondria would increase oxidative damage and further transform into large spheres, which associates with impaired mitochondrial respiration and defective organelle transport [56]. Mitochondrial fusion might represent an early response to cellular stress that provides transient protection against apoptosis and mitophage [57, 58]. Our finding on enhanced mitochondrial fusion in MCI cybrids suggests that distinct changes in mitochondrial morphology occur very early during the evolution of AD, and certainly as early as the MCI stage.

In view of the known significance of oxidative damage in the development of AD [40, 59], and the unexplored role of oxidative stress in MCI, we further explored the effect of oxidative stress on altered mitochondrial function by using the antioxidant probucol to scavenge ROS in cybrids. Our results indicate remarkable improvements in mitochondrial membrane potential, respiratory chain complex activity, and ATP production. Importantly, the elevated intracellular and mitochondria ROS production/accumulation contributes importantly to altered mitochondrial fission and fusion induced by MCI subject-derived mitochondria. Treatment of the antioxidant probucol rescued abnormal mitochondrial morphology by influencing mitochondrial fission and fusion balance and associated protein expression levels, indicating that increased oxidative stress in MCI mitochondria is responsible for perturbing mitochondrial dynamics, which in turn alters mitochondrial structure and function. The mild increase in ROS could also activate mitochondrial fusion [57, 60], aiming at compensation for the decreased mitochondrial function as observed in the MCI cases, the pre-stage of AD. Since MCI infers an increased risk of AD, antioxidant treatment that specifically target mitochondrial ROS may prove useful for MCI therapy and reduce the incidence of conversion from MCI to AD.

ROS-induced activation of the mitogen-activated protein (MAP) kinase family appears to play a key role in mediating cellular responses to multiple stresses [61]; ERK signaling is involved in mitochondrial function and neuronal stress [43, 62, 63]. In the present studies, ERK1/2 phosphorylation was significantly increased in MCI cybrids, and probucol blocked ERK1/2 activation and attenuated mitochondrial dysfunction. These data implicate a role for ERK1/2 signal transduction in altered MCI cybrid mitochondrial function.

Mitochondrial fusion may represent an early response to cellular stress [57, 58]. Up-regulated Mfn2, which should facilitate mitochondrial fusion, likely protects cells confronted by ROS accumulation [64]. Little is known about oxidative stress-associated signal transduction pathways that may regulate the mitochondrial fusion/fission dynamics in MCI subject-derived mitochondria. We reveal that blockade of ERK1/2 activation rescues mitochondrial morphology by suppressing mitochondrial Mfn2 levels in MCI cybrids. We therefore propose that Mfn2 up-regulation is induced by oxidative stress-mediated ERK activation, which in turn shifts mitochondrial dynamics towards fusion in MCI-derived

cybrids. An altered balance of mitochondrial fission and fusion is likely an important mechanism leading to mitochondrial and neuronal dysfunction in AD as well as in MCI [25]. In our previous study of AD cybrid cells, ERK inhibition restored a proper balance between mitochondrial fission and fusion, which associated with recoveries in mitochondrial morphology and function, thereby demonstrating a pivotal upstream role for ERK in the regulation of AD cybrid mitochondrial dynamics and function [40]. Here, we extend this line of investigation to MCI and find that ERK blockade improves the function of mitochondria derived from MCI subjects. This implicates a role for ERK in mediating oxidative stress-associated mitochondrial dysfunction in MCI.

Lastly, our data suggest that preventing Mfn2 overexpression in MCI reverses perturbed mitochondrial dynamics by restoring mitochondrial density and mitochondrial length. Additionally, reducing Mfn2 levels by siRNA knockdown protected neurons from MCI mitochondria-mediated injury with secondary improvements in mitochondrial respiratory function and membrane potential. These results indicate that Mfn2 plays a critical role in mitochondrial dynamic imbalance and dysfunction in MCI mitochondria.

In human AD brain and mouse models, mitochondrial morphology shifts towards excess fission [36, 50]. Similarly, results of our previous studies showed an increase in mitochondrial fission and a decrease in mitochondrial fusion in AD cybrid cells [40]. Our unexpected finding of enhanced mitochondrial fusion in MCI cybrids in the present study suggests that mitochondria may react to early stress by favoring fusion in MCI. This may suggest a strategy for differentiating between MCI and AD at the molecular level. While MCI is clinically differentiated from AD by the severity of cognitive impairment, our current study indicates that Mfn2 is paradoxically up-regulated in MCI, but down-regulated in mitochondrial fractions from AD cybrids. We hypothesize that in AD, mitochondria dynamics are decompensating and lead to deteriorating conditions in favor of fission, but in MCI, the mitochondrial fission/fusion balance leans towards fusion as a compensatory and probably reversible condition. Our findings therefore suggest that in terms of mitochondrial dynamics, MCI and AD are qualitatively different.

Taken together, we demonstrated that Mfn2 expression is markedly induced by oxidative stress-mediated ERK1/2 signal transduction and plays a critical role in promoting mitochondrial structural and functional deficits in human MCI-derived cybrid cell lines. We hypothesize that oxidative stress is an early pathological event that is present even during the MCI stage of AD. Oxidative stress-mediated activation of ERK signal transduction disrupts mitochondrial fission and fusion balance and alters mitochondrial function. Suppression of ERK signaling may restore mitochondrial morphology and functional deficits present during MCIs. Up-regulation of Mfn2, a downstream consequence of ROS-mediated ERK activation, triggers mitochondria fusion and perturbs mitochondrial dynamics (Fig. 7). Our studies suggest that the MCI stage of AD may offer unique opportunities for therapeutic development, and justify targeting oxidative stress and mitochondrial dynamics for the prevention of AD.

Supplementary Material

Refer to Web version on PubMed Central for supplementary material.

Acknowledgements

This study was supported by grants from the National Institute of Aging (R37AG037319), National institute of Neurological disorder and Stroke (NS R01NS65482), and the University of Kansas Alzheimer's Disease Center (NIA P30AG035982).

Reference

1. Petersen RC. Mild cognitive impairment: transition between aging and Alzheimer's disease. Neurologia. 2000; 15:93–101. [PubMed: 10846869]
2. Karakaya T, Fusser F, Schroder J, Pantel J. Pharmacological Treatment of Mild Cognitive Impairment as a Prodromal Syndrome of Alzheimer s Disease. Current neuropharmacology. 2013; 11:102–108. [PubMed: 23814542]
3. DeCarli C. Mild cognitive impairment: prevalence, prognosis, aetiology, and treatment. Lancet neurology. 2003; 2:15–21.
4. Bowen J, Teri L, Kukull W, McCormick W, McCurry SM, Larson EB. Progression to dementia in patients with isolated memory loss. Lancet. 1997; 349:763–765. [PubMed: 9074575]
5. Petersen RC, Stevens JC, Ganguli M, Tangalos EG, Cummings JL, DeKosky ST. Practice parameter: early detection of dementia: mild cognitive impairment (an evidence-based review). Report of the Quality Standards Subcommittee of the American Academy of Neurology. Neurology. 2001; 56:1133–1142. [PubMed: 11342677]
6. Markesbery WR, Schmitt FA, Kryscio RJ, Davis DG, Smith CD, Wekstein DR. Neuropathologic substrate of mild cognitive impairment. Archives of neurology. 2006; 63:38–46. [PubMed: 16401735]
7. Lovell MA, Markesbery WR. Oxidative DNA damage in mild cognitive impairment and late-stage Alzheimer's disease. Nucleic acids research. 2007; 35:7497–7504. [PubMed: 17947327]
8. Keller JN, Schmitt FA, Scheff SW, Ding Q, Chen Q, Butterfield DA, Markesbery WR. Evidence of increased oxidative damage in subjects with mild cognitive impairment. Neurology. 2005; 64:1152–1156. [PubMed: 15824339]
9. Migliore L, Fontana I, Trippi F, Colognato R, Coppede F, Tognoni G, Nucciarone B, Siciliano G. Oxidative DNA damage in peripheral leukocytes of mild cognitive impairment and AD patients. Neurobiology of aging. 2005; 26:567–573. [PubMed: 15708428]
10. de Leon MJ, Convit A, Wolf OT, Tarshish CY, DeSanti S, Rusinek H, Tsui W, Kandil E, Scherer AJ, Roche A, Imossi A, Thorn E, Bobinski M, Caraos C, Lesbre P, Schlyer D, Poirier J, Reisberg B, Fowler J. Prediction of cognitive decline in normal elderly subjects with 2-[(18)F]fluoro-2-deoxy-D-glucose/poitron-emission tomography (FDG/PET). Proceedings of the National Academy of Sciences of the United States of America. 2001; 98:10966–10971. [PubMed: 11526211]
11. Traykov L, Rigaud AS, Baudic S, Smagghe A, Boller F, Forette F. Apolipoprotein E epsilon 4 allele frequency in demented and cognitively impaired patients with and without cerebrovascular disease. Journal of the neurological sciences. 2002; 203–204:177–181.
12. Lopez OL, Jagust WJ, Dulberg C, Becker JT, DeKosky ST, Fitzpatrick A, Breitner J, Lyketsos C, Jones B, Kawas C, Carlson M, Kuller LH. Risk factors for mild cognitive impairment in the Cardiovascular Health Study Cognition Study: part 2. Archives of neurology. 2003; 60:1394–1399. [PubMed: 14568809]
13. Nacmias B, Piccini C, Bagnoli S, Tedde A, Cellini E, Bracco L, Sorbi S. Brain-derived neurotrophic factor, apolipoprotein E genetic variants and cognitive performance in Alzheimer's disease. Neuroscience letters. 2004; 367:379–383. [PubMed: 15337270]
14. Swerdlow RH, Khan SMA. "mitochondrial cascade hypothesis" for sporadic Alzheimer's disease. Medical hypotheses. 2004; 63:8–20. [PubMed: 15193340]

15. Valla J, Schneider L, Niedzielko T, Coon KD, Caselli R, Sabbagh MN, Ahern GL, Baxter L, Alexander G, Walker DG, Reiman EM. Impaired platelet mitochondrial activity in Alzheimer's disease and mild cognitive impairment. Mitochondrion. 2006; 6:323–330. [PubMed: 17123871]
16. Silva DF, Santana I, Esteves AR, Baldeiras I, Arduino DM, Oliveira CR, Cardoso SM. Prodromal metabolic phenotype in MCI cybrids: implications for Alzheimer's disease. Current Alzheimer research. 2013; 10:180–190. [PubMed: 22746213]
17. Smirnova E, Griparic L, Shurland DL, van der Bliek AM. Dynamin related protein Drp1 is required for mitochondrial division in mammalian cells. Molecular biology of the cell. 2001; 12:2245–2256. [PubMed: 11514614]
18. Chen HC, Detmer SA, Ewald AJ, Griffin EE, Fraser SE, Chan DC. Mitofusins Mfn1 and Mfn2 coordinately regulate mitochondrial fusion and are essential for embryonic development. Journal of Cell Biology. 2003; 160:189–200. [PubMed: 12527753]
19. Detmer SA, Chan DC. Functions and dysfunctions of mitochondrial dynamics. Nature reviews. Molecular cell biology. 2007; 8:870–879.
20. Song ZY, Ghochani M, McCaffery JM, Frey TG, Chan DC. Mitofusins and OPA1 Mediate Sequential Steps in Mitochondrial Membrane Fusion. Molecular biology of the cell. 2009; 20:3525–3532. [PubMed: 19477917]
21. Hollenbeck PJ, Saxton WM. The axonal transport of mitochondria. Journal of cell science. 2005; 118:5411–5419. [PubMed: 16306220]
22. Chen HC, McCaffery JM, Chan DC. Mitochondrial fusion protects against neurodegeneration in the cerebellum. Cell. 2007; 130:548–562. [PubMed: 17693261]
23. Verstreken P, Ly CV, Venken KJT, Koh TW, Zhou Y, Bellen HJ. Synaptic mitochondria are critical for mobilization of reserve pool vesicles at Drosophila neuromuscular junctions. Neuron. 2005; 47:365–378. [PubMed: 16055061]
24. Corrado M, Scorrano L, Campello S. Mitochondrial dynamics in cancer and neurodegenerative and neuroinflammatory diseases. International journal of cell biology. 2012; 2012:729290. [PubMed: 22792111]
25. Wang X, Su B, Lee HG, Li X, Perry G, Smith MA, Zhu X. Impaired balance of mitochondrial fission and fusion in Alzheimer's disease. The Journal of neuroscience : the official journal of the Society for Neuroscience. 2009; 29:9090–9103. [PubMed: 19605646]
26. Manczak M, Calkins MJ, Reddy PH. Impaired mitochondrial dynamics and abnormal interaction of amyloid beta with mitochondrial protein Drp1 in neurons from patients with Alzheimer's disease: implications for neuronal damage. Human molecular genetics. 2011; 20:2495–2509. [PubMed: 21459773]
27. Wang X, Su B, Siedlak SL, Moreira PI, Fujioka H, Wang Y, Casadesus G, Zhu X. Amyloid-beta overproduction causes abnormal mitochondrial dynamics via differential modulation of mitochondrial fission/fusion proteins. Proceedings of the National Academy of Sciences of the United States of America. 2008; 105:19318–19323. [PubMed: 19050078]
28. Calkins MJ, Manczak M, Mao P, Shirendeb U, Reddy PH. Impaired mitochondrial biogenesis, defective axonal transport of mitochondria, abnormal mitochondrial dynamics and synaptic degeneration in a mouse model of Alzheimer's disease. Human molecular genetics. 2011; 20:4515–4529. [PubMed: 21873260]
29. Albert MS, DeKosky ST, Dickson D, Dubois B, Feldman HH, Fox NC, Gamst A, Holtzman DM, Jagust WJ, Petersen RC, Snyder PJ, Carrillo MC, Thies B, Phelps CH. The diagnosis of mild cognitive impairment due to Alzheimer's disease: recommendations from the National Institute on Aging-Alzheimer's Association workgroups on diagnostic guidelines for Alzheimer's disease. Alzheimer's & dementia : the journal of the Alzheimer's Association. 2011; 7:270–279.
30. Swerdlow RH. Mitochondria in cybrids containing mtDNA from persons with mitochondriopathies. Journal of neuroscience research. 2007; 85:3416–3428. [PubMed: 17243174]
31. Du H, Guo L, Fang F, Chen D, Sosunov AA, McKhann GM, Yan Y, Wang C, Zhang H, Molkentin JD, Gunn Moore FJ, Vonsattel JP, Arancio O, Chen JX, Yan SD. Cyclophilin D deficiency attenuates mitochondrial and neuronal perturbation and ameliorates learning and memory in Alzheimer's disease. Nature medicine. 2008; 14:1097–1105.

32. Takuma K, Yao J, Huang J, Xu H, Chen X, Luddy J, Trillat AC, Stern DM, Arancio O, Yan SS. ABAD enhances Abeta induced cell stress via mitochondrial dysfunction. FASEB journal : official publication of the Federation of American Societies for Experimental Biology. 2005; 19:597–598. [PubMed: 15665036]
33. Mancuso M, Filosto M, Bosetti F, Ceravolo R, Rocchi A, Tognoni G, Manca ML, Solaini G, Siciliano G, Murri L. Decreased platelet cytochrome c oxidase activity is accompanied by increased blood lactate concentration during exercise in patients with Alzheimer disease. Experimental neurology. 2003; 182:421–426. [PubMed: 12895452]
34. Graham S, Gorin Y, Abboud HE, Ding M, Lee DY, Shi H, Ding Y, Ma R. Abundance of TRPC6 protein in glomerular mesangial cells is decreased by ROS and PKC in diabetes. American journal of physiology. Cell physiology. 2011; 301:C304–C315. [PubMed: 21525431]
35. Yan SD, Yan SF, Chen X, Fu J, Chen M, Kuppusamy P, Smith MA, Perry G, Godman GC, Nawroth P, et al. Non enzymatically glycated tau in Alzheimer's disease induces neuronal oxidant stress resulting in cytokine gene expression and release of amyloid beta-peptide. Nat Med. 1995; 1:693–699. [PubMed: 7585153]
36. Lustbader JW, Cirilli M, Lin C, Xu HW, Takuma K, Wang N, Caspersen C, Chen X, Pollak S, Chaney M, Trinchese F, Liu S, Gunn-Moore F, Lue LF, Walker DG, Kuppusamy P, Zewier ZL, Arancio O, Stern D, Yan SS, Wu H. ABAD directly links Abeta to mitochondrial toxicity in Alzheimer's disease. Science. 2004; 304:448–452. [PubMed: 15087549]
37. Wang X, Su B, Zheng L, Perry G, Smith MA, Zhu X. The role of abnormal mitochondrial dynamics in the pathogenesis of Alzheimer's disease. Journal of neurochemistry. 2009; 109(Suppl 1):153–159. [PubMed: 19393022]
38. Mozdy AD, Shaw JM. A fuzzy mitochondrial fusion apparatus comes into focus. Nature reviews. Molecular cell biology. 2003; 4:468–478.
39. Reddy PH, Tripathi R, Troung Q, Tirumala K, Reddy TP, Anekonda V, Shirendeb UP, Calkins MJ, Reddy AP, Mao P, Manczak M. Abnormal mitochondrial dynamics and synaptic degeneration as early events in Alzheimer's disease: implications to mitochondria-targeted antioxidant therapeutics. Biochimica et biophysica acta. 2012; 1822:639–649. [PubMed: 22037588]
40. Gan X, Huang S, Wu L, Wang Y, Hu G, Li G, Zhang H, Yu H, Swerdlow RH, Chen JX, Yan SS. Inhibition of ERK-DLP1 signaling and mitochondrial division alleviates mitochondrial dysfunction in Alzheimer's disease cybrid cell. Biochimica et biophysica acta. 2013; 1842:220–231. [PubMed: 24252614]
41. Yu T, Robotham JL, Yoon Y. Increased production of reactive oxygen species in hyperglycemic conditions requires dynamic change of mitochondrial morphology. Proceedings of the National Academy of Sciences of the United States of America. 2006; 103:2653–2658. [PubMed: 16477035]
42. Guo L, Du H, Yan S, Wu X, McKhann GM, Chen JX, Yan SS. Cyclophilin D deficiency rescues axonal mitochondrial transport in Alzheimer's neurons. PloS one. 2013; 8:e54914. [PubMed: 23382999]
43. Arancio O, Zhang HP, Chen X, Lin C, Trinchese F, Puzzo D, Liu S, Hegde A, Yan SF, Stern A, Luddy JS, Lue LF, Walker DG, Roher A, Buttini M, Mucke L, Li W, Schmidt AM, Kindy M, Hyslop PA, Stern DM, Du Yan SS. RAGE potentiates Abeta-induced perturbation of neuronal function in transgenic mice. Embo J. 2004; 23:4096–4105. [PubMed: 15457210]
44. Du H, Guo L, Wu X, Sosunov AA, McKhann GM, Chen JX, Yan SS. Cyclophilin D deficiency rescues Abeta-impaired PKA/CREB signaling and alleviates synaptic degeneration. Biochimica et biophysica acta. 2013
45. Yu T, Jhun BS, Yoon Y. High-glucose stimulation increases reactive oxygen species production through the calcium and mitogen-activated protein kinase-mediated activation of mitochondrial fission. Antioxidants & redox signaling. 2011; 14:425–437. [PubMed: 20518702]
46. Fan C, Chen J, Wang Y, Wong YS, Zhang Y, Zheng W, Cao W, Chen T. Selenocystine potentiates cancer cell apoptosis induced by 5-fluorouracil by triggering reactive oxygen species mediated DNA damage and inactivation of the ERK pathway. Free radical biology & medicine. 2013; 65:305–316. [PubMed: 23837948]

47. Wang X, Liu JZ, Hu JX, Wu H, Li YL, Chen HL, Bai H, Hai CX. ROS-activated p38 MAPK/ERK Akt cascade plays a central role in palmitic acid-stimulated hepatocyte proliferation. Free radical biology & medicine. 2011; 51:539–551. [PubMed: 21620957]

48. Misko A, Jiang SR, Wegorzewska I, Milbrandt J, Baloh RH. Mitofusin 2 Is Necessary for Transport of Axonal Mitochondria and Interacts with the Miro/Milton Complex. J Neurosci. 2010; 30:4232–4240. [PubMed: 20335458]

49. Caspersen C, Wang N, Yao J, Sosunov A, Chen X, Lustbader JW, Xu HW, Stern D, McKhann G, Yan SD. Mitochondrial Abeta: a potential focal point for neuronal metabolic dysfunction in Alzheimer's disease. FASEB journal : official publication of the Federation of American Societies for Experimental Biology. 2005; 19:2040–2041. [PubMed: 16210396]

50. Du H, Yan SS. Mitochondrial medicine for neurodegenerative diseases. The international journal of biochemistry & cell biology. 2010; 42:560–572. [PubMed: 20067840]

51. DeKosky ST, Marek K. Looking backward to move forward: early detection of neurodegenerative disorders. Science. 2003; 302:830–834. [PubMed: 14593169]

52. Silva DF, Selfridge JE, Lu J, E L, Roy N, Hutfles L, Burns JM, Michaelis EK, Yan S, Cardoso SM, Swerdlow RH. Bioenergetic flux, mitochondrial mass and mitochondrial morphology dynamics in AD and MCI cybrid cell lines. Human molecular genetics. 2013; 22:3931–3946. [PubMed: 23740939]

53. Liang H, Ward WF. PGC-1alpha: a key regulator of energy metabolism. Advances in physiology education. 2006; 30:145–151. [PubMed: 17108241]

54. Leone TC, Lehman JJ, Finck BN, Schaeffer PJ, Wende AR, Boudina S, Courtois M, Wozniak DF, Sambandam N, Bernal Mizrachi C, Chen Z, Holloszy JO, Medeiros DM, Schmidt RE, Saffitz JE, Abel ED, Semenkovich CF, Kelly DP. PGC 1alpha deficiency causes multi system energy metabolic derangements: muscle dysfunction, abnormal weight control and hepatic steatosis. PLoS biology. 2005; 3:e101. [PubMed: 15760270]

55. Chen H, Chan DC. Mitochondrial dynamics--fusion, fission, movement, and mitophagy--in neurodegenerative diseases. Human molecular genetics. 2009; 18:R169–R176. [PubMed: 19808793]

56. Chan DC. Mitochondria: dynamic organelles in disease, aging, and development. Cell. 2006; 125:1241–1252. [PubMed: 16814712]

57. Tondera D, Grandemange S, Jourdain A, Karbowski M, Mattenberger Y, Herzig S, Da Cruz S, Clerc P, Raschke I, Merkwirth C, Ehses S, Krause F, Chan DC, Alexander C, Bauer C, Youle R, Langer T, Martinou JC. SLP-2 is required for stress induced mitochondrial hyperfusion. The EMBO journal. 2009; 28:1589–1600. [PubMed: 19360003]

58. Rambold AS, Kostelecky B, Elia N, Lippincott Schwartz J. Tubular network formation protects mitochondria from autophagosomal degradation during nutrient starvation. Proceedings of the National Academy of Sciences of the United States of America. 2011; 108:10190–10195. [PubMed: 21646527]

59. Zhu X, Raina AK, Lee HG, Casadesus G, Smith MA, Perry G. Oxidative stress signalling in Alzheimer's disease. Brain research. 2004; 1000:32–39. [PubMed: 15053949]

60. Shutt T, Geoffrion M, Milne R, McBride HM. The intracellular redox state is a core determinant of mitochondrial fusion. Embo Rep. 2012; 13:909–915. [PubMed: 22945481]

61. Johnson GL, Lapadat R. Mitogen-activated protein kinase pathways mediated by ERK, JNK, and p38 protein kinases. Science. 2002; 298:1911–1912. [PubMed: 12471242]

62. Dong XB, Yang CT, Zheng DD, Mo LQ, Wang XY, Lan AP, Hu F, Chen PX, Feng JQ, Zhang MF, Liao XX. Inhibition of ROS-activated ERK1/2 pathway contributes to the protection of H2S against chemical hypoxia induced injury in H9c2 cells. Molecular and cellular biochemistry. 2012; 362:149–157. [PubMed: 22134701]

63. Rasola A, Sciacovelli M, Chiara F, Pantic B, Brusilow WS, Bernardi P. Activation of mitochondrial ERK protects cancer cells from death through inhibition of the permeability transition. Proc Natl Acad Sci U S A. 2010; 107:726–731. [PubMed: 20080742]

64. Sugioka R, Shimizu S, Tsujimoto Y. Fzo1, a protein involved in mitochondrial fusion, inhibits apoptosis. The Journal of biological chemistry. 2004; 279:52726–52734. [PubMed: 15459195]

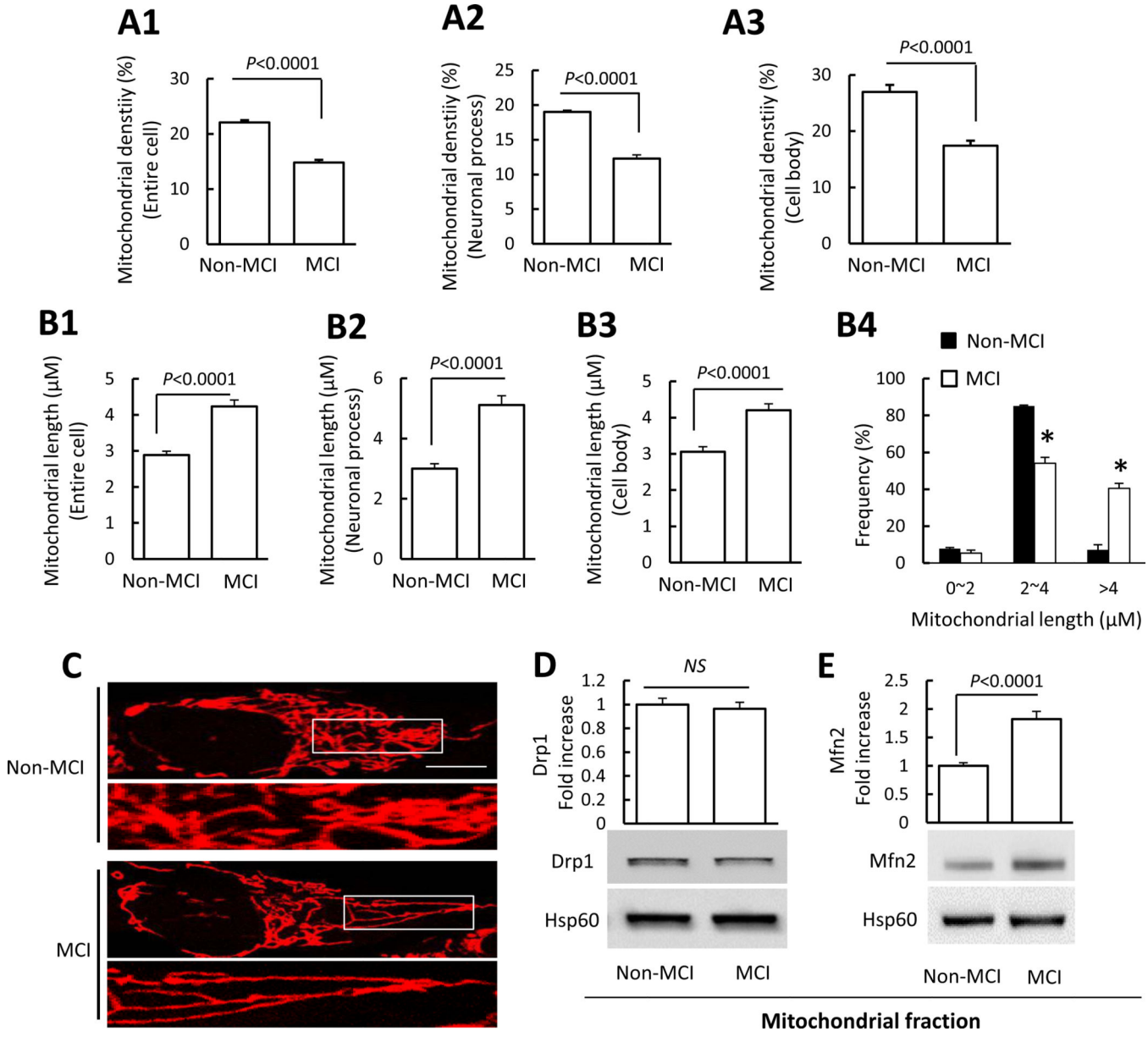

Figure 1.

Abnormal mitochondrial morphology in MCI cybrid cells. Cybrid cells were labeled with Mitotracker Red for visualization of mitochondrial morphology. **(A1–A3)** Quantitative measurement of mitochondrial density (using NIH ImageJ software) presented as the percentage of area occupied by mitochondria in entire cells (**A1**), neuronal process (**A2**), or cell body (**A3**). (**B1–B3**) Average mitochondrial length throughout the entire cell, neuronal processes, and cell body was higher in MCI cybrid cells compared to Non-MCI cells. (**B4**) Quantification of mitochondrial size based on the grouped differently sized bins. (**C**) Representative images of Mitotracker Red staining. Lower panels present larger images corresponding to the indicated images above. Scale bar = 5 μm. N = 7 cell lines/group. (**D–E**) Drp1 and Mfn2 expression levels in Non-MCI and MCI cybrid mitochondria. Densitometry of immunoreactive bands for Drp1 (**D**) and Mfn2 (**E**) in mitochondrial

fractions of the indicated groups of cybrid cells. Data are expressed as fold-increase of Drp1 or Mfn2 relative to Non-MCI cells. Drp1 andMfn2 levels were normalized to mitochondrial marker Hsp60. Representative immunoblots are shown underneath. N = 7 cell lines/group.

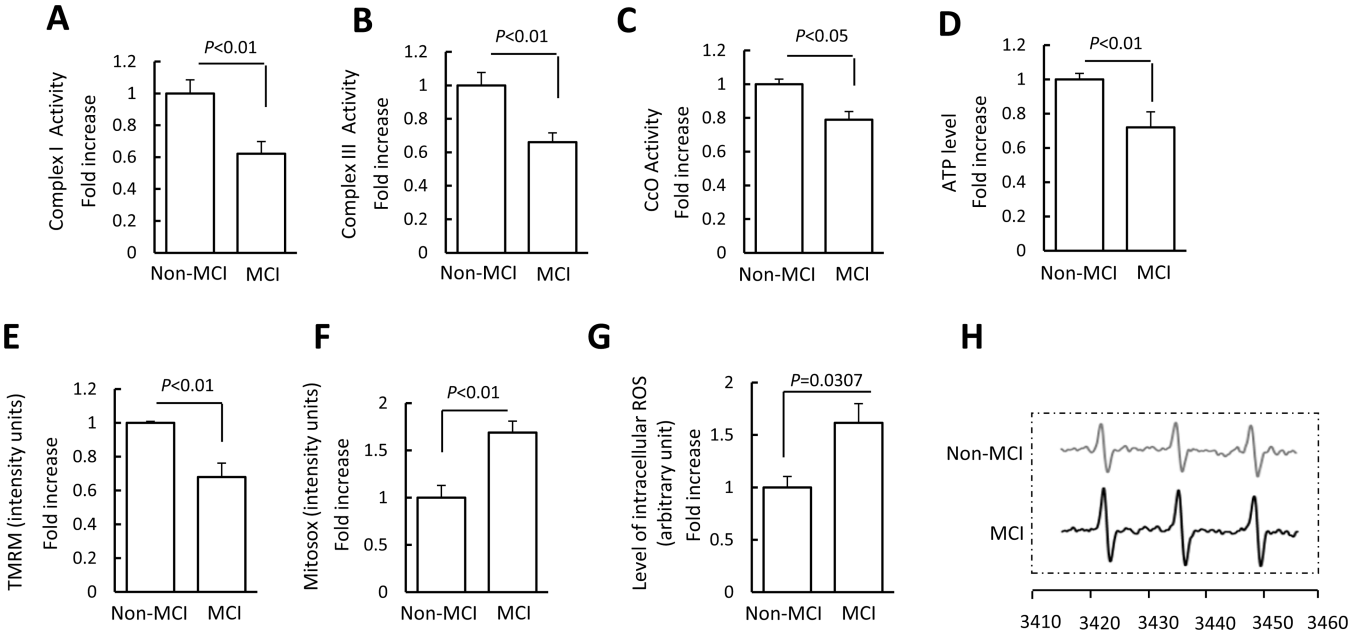

Figure 2.

Mitochondrial dysfunction in MCI cybrid cells. **(A–D)** Enzymatic activity of complex I, III, and IV (CcO), and ATP levels were determined in cell lysates from indicated cell groups. (**E–F)** Mitochondrial membrane potential and reactive oxygen species (ROS) were measured by tetramethylrhodamine methyl ester (TMRM) (**E**) and Mitosox staining intensity (**F**), respectively. Image intensity was quantified using NIH ImageJ software. (**G**) The production of the intracellular ROS determined by EPR spectroscopy in Non-MCI and MCI cybrids. (**H**) Representative spectra of EPR. The peak height in the spectrum indicates the level of reactive oxygen species (ROS). Data are expressed as fold increase relative to Non-MCI cybrid cells. N = 7 cell lines/group.

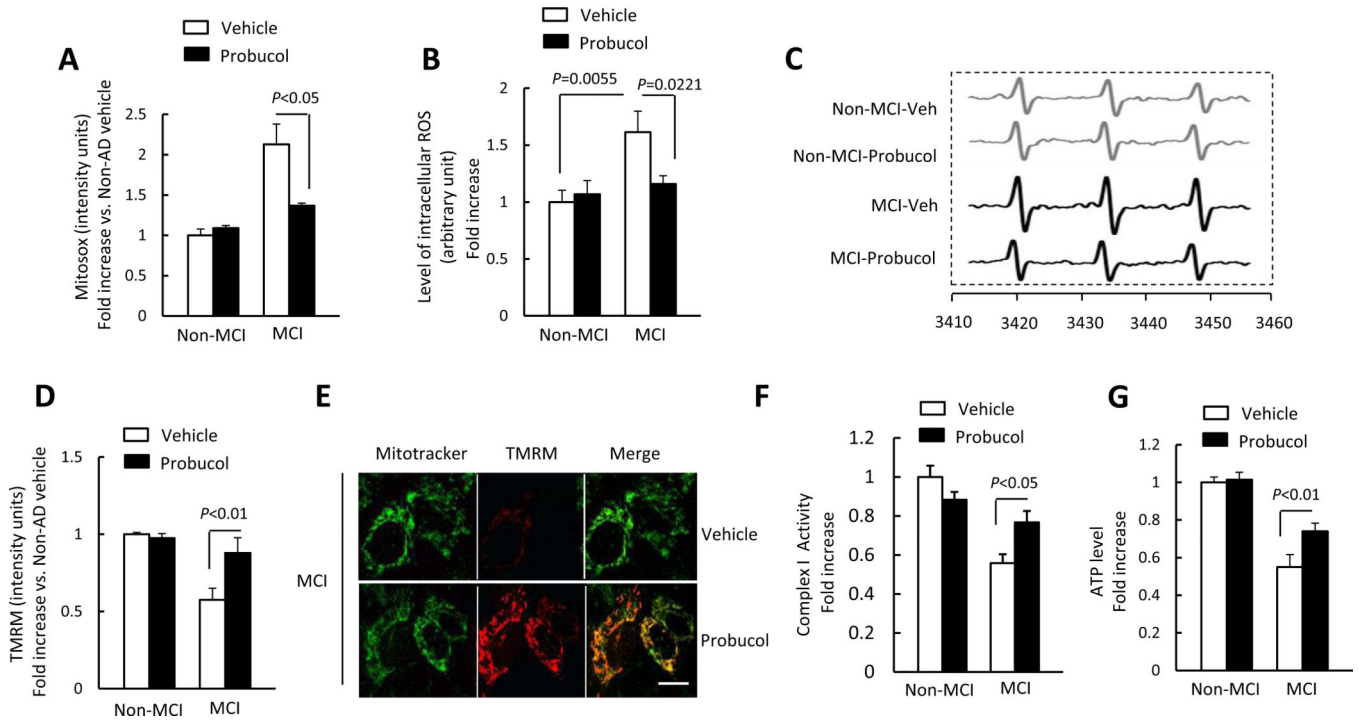

Figure 3.

Effect of antioxidant treatment on mitochondrial function and morphology. (**A–C)** Cells were treated with probucol (10 μM) for 24 h and then stained with Mitosox to determine mitochondrial ROS levels, or tested EPR values to evaluate intracellular ROS production. Quantification of staining intensity for Mitosox (**A**), EPR values (**B**), and representative EPR spectra (**C**). Mitochondrial membrane potential was shown as the quantification of staining intensity of TMRM (**D**) and representative images with TMRM staining (Scale bar = 10 μm) (**E**). (**F–G)** Complex I activity (**F**) and ATP levels (**G**) were measured in the indicated groups of cells with or without probucol treatment. Data are expressed as fold increase relative to vehicle treated Non-MCI cybrid cells. N = 7 cell lines/group.

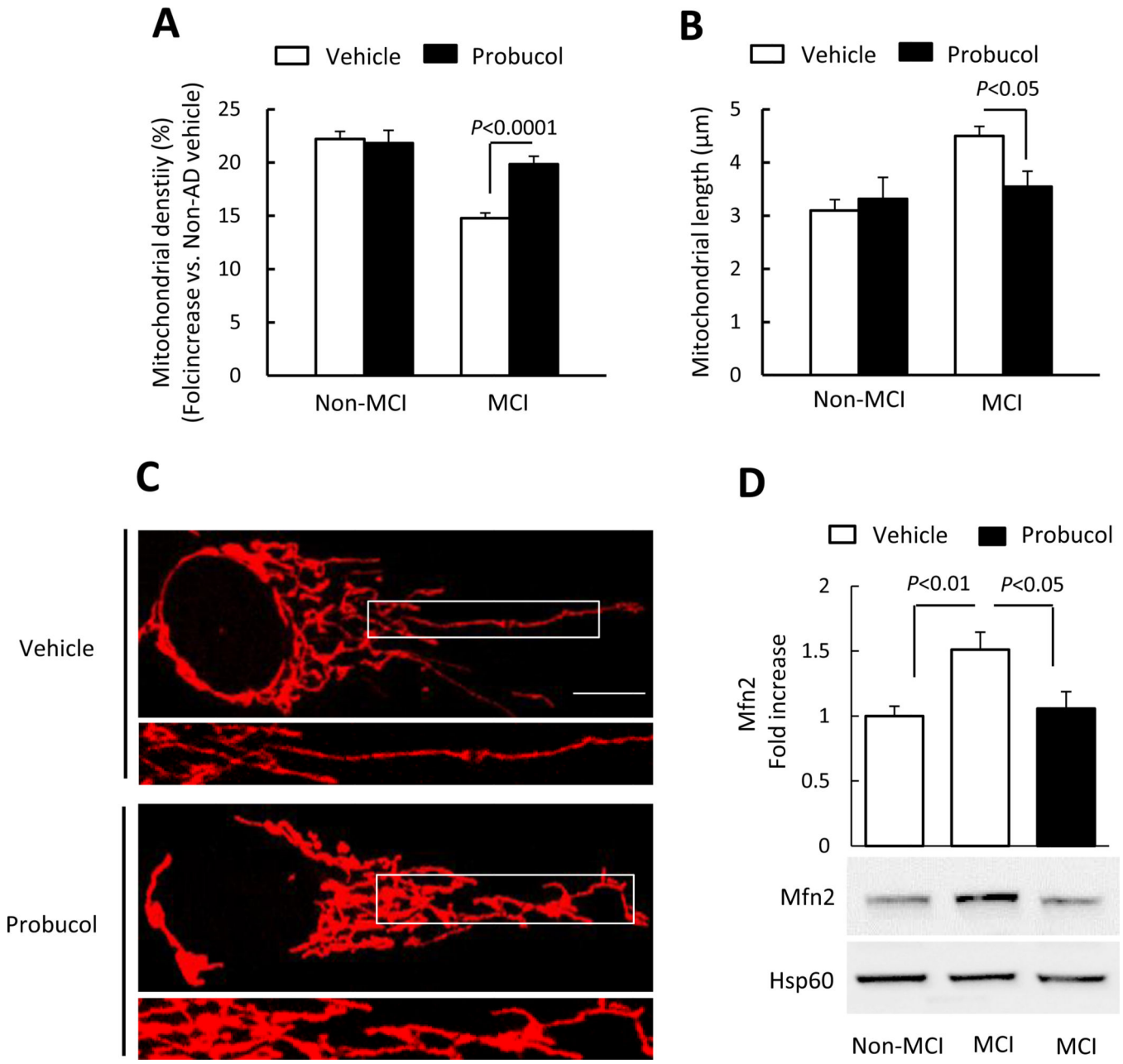

Figure 4.

(**A–B)** Quantitative measurement of mitochondrial density (**A**) and average mitochondrial length (**B**) in the indicated cell groups using NIH ImageJ software. (**C**) Representative images of Mitotracker Red staining. Lower panels present larger images corresponding to the indicated images above (Scale bar = 5μM). (**D**) Quantification of immunoreactive bands for Mfn2 relative to Hsp60 in the indicated cell groups with probucol or vehicle treatment using NIH ImageJ software. Data are expressed as fold increase relative to vehicle-treated Non-MCI cybrid cells. Representative immunoblots are shown in the lower panel. N = 5–7 cell lines/group.

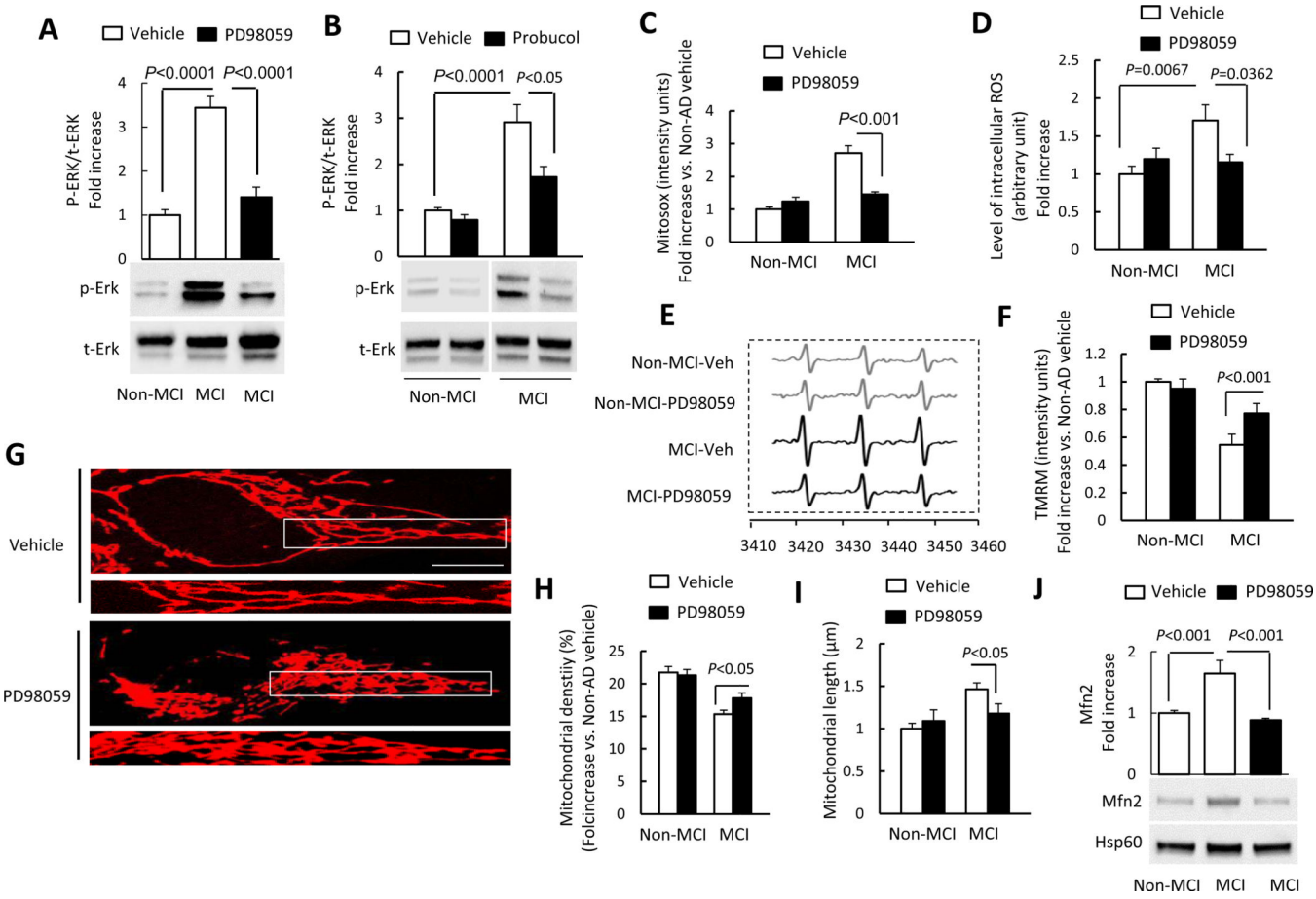

Figure 5.

Inhibition of ERK activation rescued abnormal mitochondrial function and morphology. (**A–B)** Densitometry of immunoreactive bands for phospho-ERK1/2 (p-ERK1/2) using NIH Image J software, normalized to total-ERK1/2 (t-ERK1/2) in indicated cell groups treated with PD98059 (10 μM for 2 h) (**A**), probucol (10 μM for 24 h) (**B**), or vehicle. Representative immunoblots are shown in lower panel. **(C)** PD98059 treatment decreased Mitosox staining intensity in MCI cybrid cells compared to vehicle treatment. (**D–E**) PD98059 treatment decreased intracellular ROS production in MCI cybrids compared to vehicle treatment measured by EPR. Quantification of EPR values in the indicated cybrid cells (**D**). (**E**) Representative EPR spectra. (**F**) TMRM staining intensity was significantly increased in MCI cybrid cells treated with PD98059. (**G–I)** Effects of ERK inhibitor on mitochondrial morphology. Representative images are shown for Mitotracker Red staining. The lower panel is a larger image corresponding to the indicated image above (Scale bar = 5 μm) (**G**). Mitochondrial density (**H**) and average length (**I**) were measured in the indicated cell groups treated with PD98059 or vehicle. (**J)** Quantification of immunoreactive bands for Mfn2 normalized to Hsp60 in mitochondrial fractions of the indicated cell group with PD98059 or vehicle treatment. Representative immunoblots are shown in lower panel. Data are expressed as fold increase relative to vehicle-treated Non-MCI cybrid cells. N = 5–7 cell lines/group.

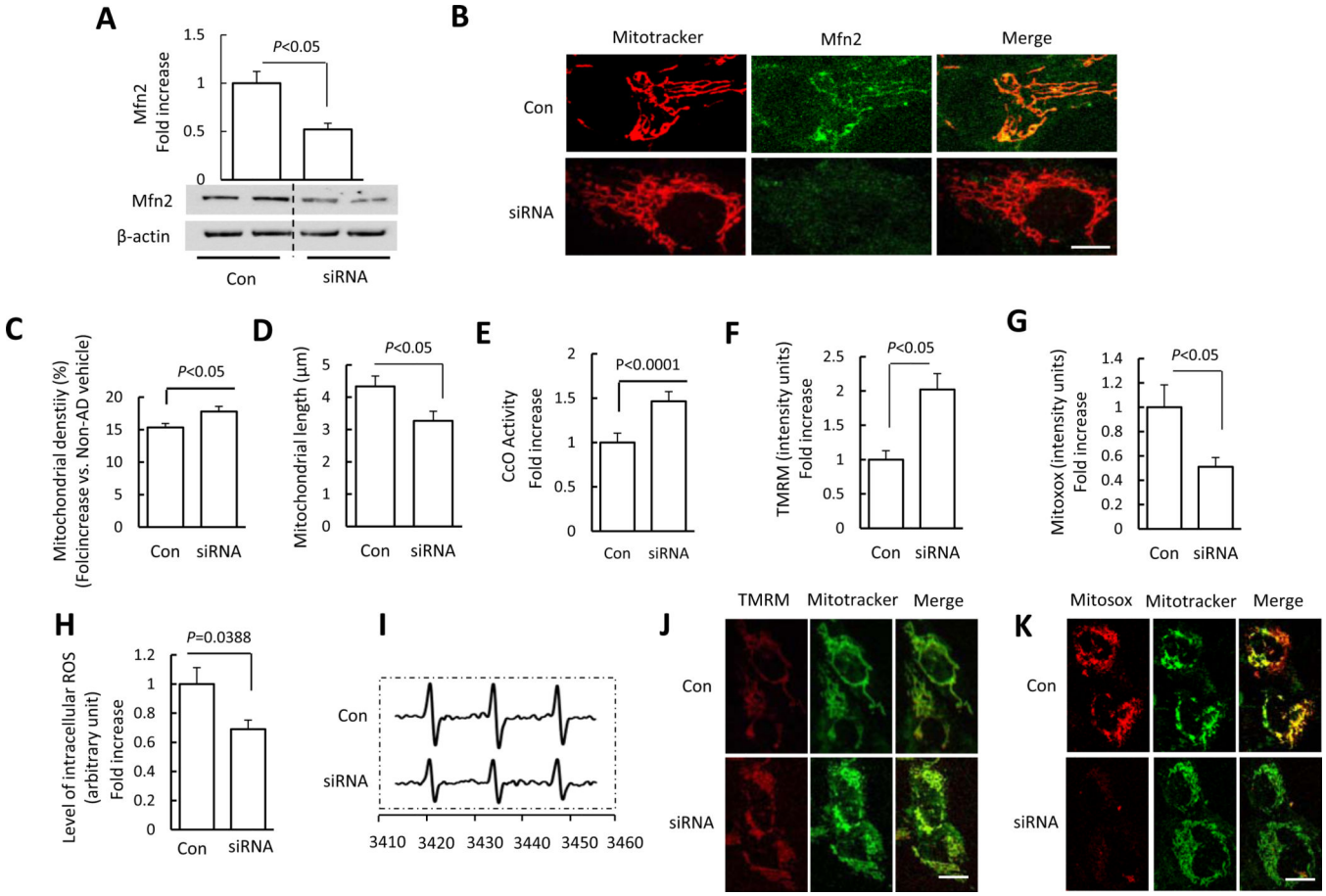

Figure 6.

Effect of Mfn2 blockade on MCI mitochondrial morphology and function. (**A)** Quantification of immunoreactive bands for Mfn2 normalized to β-actin in MCI cybrid cell lysate of the indicated group with siRNA-control and siRNA-Mfn2 transfection. Representative immunoblots are shown in the lower panel. Data are expressed as fold increase relative to siRNA-control transfected MCI cybrid cells. (**B**) MCI cybrid cells were transfected with siRNA-control or siRNA-Mfn2. After 24 h, cells were incubated with Mitotracker Red to analyze mitochondrial morphology using confocal microscopy (Scale bar = 5 μm). siRNA-Mfn2 transfected MCI cybrids had tubular mitochondria, whereas siRNA-control transfected cells retained elongated mitochondrial morphology. Mitochondrial average density (**C**), length (**D**), and CcO activity (**E**), and mitochondrial membrane potential (TMRM) (**F**) were restored in siRNA-Mfn2 transfected cells compared to siRNA- transfected control cells. ROS production measured by Mitosox (**G**) and EPR values (**H, I**) were suppressed in siRNA-Mfn2 transfected cells compared to siRNA-transfected control cells. (**H**) Quantification of EPR values in the indicated groups of cells. (**I**) Representative EPR spectra. (**J,K**) Representative images for Mitotracker and Mitosox staining are shown (Scale bar = 10 μm). N = 5–7 cell lines/group.

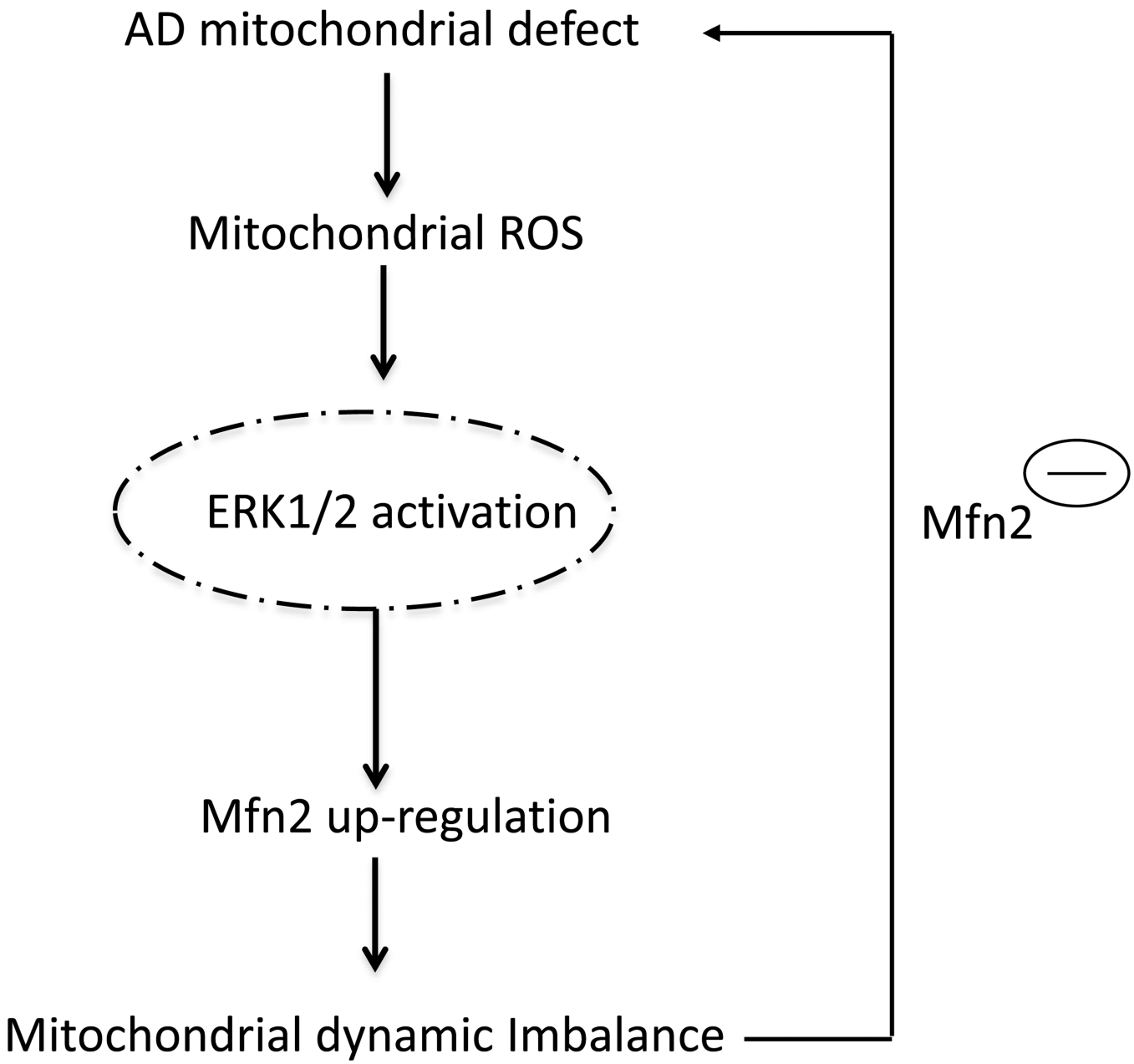

Figure 7.

Schematic diagram showing sequence in which defects in MCI mitochondrial respiratory function result in increased mitochondrial ROS generation/accumulation stems; this in turn leads to activation of ERK signal transduction. ERK activation directly or indirectly disrupts the balance of mitochondrial dynamics (fusion and fission events) and results in altered Mfn2 expression levels, eventually leading to aberrant mitochondrial morphology and function. Genetic knockdown of Mfn2 expression rescues perturbation of mitochondrial morphology and function relevant to MCI mitochondrial degeneration.